Journal of
Ceramic Science
and Technology

Alkali-Activated Materials Based on Callovo-Oxfordian Argillite: Formation, Structure and Mechanical Properties

C. Dupuy[1, 2], A. Gharzouni[2], N. Texier-Mandoki[1], X. Bourbon[1], S. Rossignol[*2]

[1]Agence nationale pour la gestion des déchets radioactifs (ANDRA), 1/7 rue Jean-Monnet 92298 Chatenay-Malabry Cedex, France.
[2]Institut de Recherche sur les Céramiques (IRCER), 12 rue Atlantis, 87068 Limoges Cedex, France

Abstract

If accepted, the construction of Cigéo, a French geological disposal facility for radioactive waste, will lead to the excavation of a large quantity of Callovo-Oxfordian (COx) argillite. The valorization of this raw material by alkaline activation was studied. For this, COx argillite without and with thermal treatment at 750 °C using furnace and flash processes were investigated. These treatments led mainly to the dehydroxylation of clay minerals and the decomposition of carbonate compounds. The feasibility of the alkali-activated samples based on different argillite samples and their mixtures was evaluated. Then, the consolidated samples were characterized by FTIR, X-ray diffraction, thermal analysis and compressive strength measurements. The results demonstrate that alkali activation is possible for all samples that contain at least 25 % calcined argillite (using both furnace and flash treatments). However, only samples without raw argillite indicate the formation of a geopolymer network and exhibit sufficient compressive strength. Lastly, the decomposition of the carbonate species (which produces free calcium and magnesium) was further studied. Indeed, the free alkaline earth cations led to structural modification in the alkali-activated samples.

Keywords: Callovo-Oxfordian, argillite, alkali-activated, heat treatment, carbonate, calcium

I. Introduction

High-level and intermediate-level long-lived wastes are the main products issued mainly from the nuclear industry and especially from the reprocessing of the nuclear spent fuel. The activity level and long half-lives of the waste justify deep geological disposal to ensure their confinement over several hundreds of thousands of years. In France, the French National Radioactive Waste Management Agency (Andra) is currently investigating the feasibility of a geological disposal site, called Cigéo, in eastern France between the Meuse and the Haute-Marne. The host geological layer, called Callovo-Oxfordian (COx) argillite, is located approximately 500 m under the ground level [1, 2]. If the construction of the disposal facility is accepted by the French authorities, the digging of the facilities will lead to the excavation of a total of millions of cubic meters of COx argillite, all along the Cigeo operating period (i.e., 100 years). Part of the excavated argillite will be used as backfill material. However, others methods for valorization are currently being assessed. In this study, the alkali-activation of COx argillite is investigated. The main mineral phases in COx argillite are clay minerals, but a high rate of carbonates and tectosilicates are also present [1].

Alkali-activated materials were introduced by Glukhovsky in 1957 and are more commonly called geopolymers (which is a subgroup of the alkali-activated materials). These materials are amorphous inorganic materials shaped at low temperature (< 100 °C) by the activation of an aluminosilicate source by an alkaline silicate solution [3, 4]. One advantage of these materials is the variety of aluminosilicate sources suitable for alkali activation. The possible use of crude aluminosilicate sources (without thermal treatment) has been demonstrated [5]. However, better working properties of the final synthesized materials were generally obtained using thermally treated aluminosilicate sources [6, 7]. Indeed, the thermal treatment induces the dehydroxylation of the clay minerals and a disorganization of the structure. Thermal treatment also leads to other transformations mainly on the carbonate species [8]. Recently, Gharzouni *et al.* [8] have studied the structural variations induced by the thermal treatment of argillite at different temperatures using furnace and flash processes to develop the alkali-activated materials. Gharzouni and coworkers demonstrated that at a temperature of 750 °C, furnace calcination leads to more complete clay mineral dehydroxylation and carbonate decomposition than does flash processing at the same temperature.

Particular interest is given to the decomposition of calcium carbonate, which results in the formation of lime and strongly influences the alkaline activation. Indeed, the presence of reactive calcium (free lime) in the mixture leads to a modification of the kinetics of polycondensation by decreasing the setting time [9]. Moreover, the structure of the final materials can be different with the appearance of

---

* Corresponding author: sylvie.rossignol@unilim.fr

a C-S-H phase due to the presence of large amounts of free lime and silica in this alkaline medium (this reaction is known as a pozzolanic reaction leading to the formation of C-S-H) [10, 11]. Moreover, the presence of calcium in the reactive mixture can also interfere with the geopolymerization reaction, which leads to Si-O-Ca bond formation [12]. Lastly, the carbonates can react with hydrated lime to form calcium carbonate [11, 13].

Despite the existing literature, the evolution of different carbonate compounds during alkali-activation is still not well understood and strongly depends on the raw materials that are used. The objective of this study is to investigate the formation, structure and mechanical properties of alkali-activated materials based on COx argillite and to focus on the evolution of the carbonate species. To do this, two different calcination processes (furnace and flash calcinations) and mixtures of raw and calcined argillite are studied. The study of various mixtures with different degrees of carbonate decomposition will allow a better understanding of the effect of calcium on alkali-activated samples based on COx argillite.

II. Experimental

(1) Raw materials

The COx argillite formation, where the Cigeo facilities will be implemented, is composed of 52 % clay minerals (interlayered illite/smectite, illite, kaolinite and chlorite), 26 % carbonate (calcite and dolomite) and 17 % quartz [1, 2]. The other components are mainly feldspar and pyrite. The chemical composition is reported in Table 1. The samples of argillite were ground and calcined in two different processes (furnace and flash), as described by A. Gharzouni et al. [8]. The furnace process is a classic calcination of the powder for four hours in a laboratory furnace, and the flash process consists of a very short exposure of the powder (by an airflow circulation) to a flame. In this paper, three different argillite powders were used: Ar (raw argillite), Ac (furnace-calcined argillite at 750 °C) and Af (flash-calcined argillite at 750 °C).

(2) Sample preparation

The consolidated samples were synthesized by mixing the powders of argillites with a potassium alkaline silicate solution (58 % water, and the molar ratio of Si/K = 0.58). The blends were cast in a closed polystyrene mold and maintained at room temperature for seven days (a classic procedure in the laboratory). The alkali-activated samples were referred to by the letter G, which is a reference to the raw materials. When several raw materials were used, the

notation of the raw material was completed by the weight percent of each material. For example, $GAr_{0.5}Ac_{0.5}$ is a consolidated sample based on 50 % raw argillite and 50 % calcined argillite.

(3) Sample characterization

Differential thermal analysis (DTA) and thermogravimetric analysis (TGA) were conducted with an SDT Q600, TA Instruments. Measurements were performed under a dry airflow (100 mL/min) in a platinum crucible. The samples were heated to 1200 °C at a rate of 5 °C/min. In addition, DTA-TGA coupled with mass spectrometry was performed with a Netzsch STA 449F3 analyzer. For these measurements, the samples were heated to 1200 °C at a rate of 10 °C/min under an argon flow. Only the H_2O (m/z = 18), CO_2 (m/z = 44) and SO_2 (m/z = 64) curves were selected from previous studies [8]. The apparatus does not allow quantitative measurements.

X-ray diffraction (XRD) patterns were obtained with a Bruker-D8 Advance diffractometer with a Bragg-Brentano geometry and a $CuK\alpha_1\alpha_2$ detector. The analytical range is between 5 ° and 55 ° (2θ) with a step width of 0.02 ° (2θ) and a dwell time of 1 s. Phase identification was performed with Joint Committee on Powder Diffraction Standards (JCPDS). A quantitative analysis was conducted via the Rietveld method using Topas software. For these measurements, the sample was mixed with 30 % ZnO.

Fourier-transform infrared (FTIR) spectra were obtained with a Thermo Fisher Scientific Nicolet 380 with an attenuated total reflectance (ATR) module. The spectra were recorded between 400 and 4000 cm⁻¹ at a resolution of 4 cm⁻¹, and 64 scans were conducted. Atmospheric CO_2 was removed between 2280 and 2400 cm⁻¹ and replaced by a straight line [14]. FTIR measurements were used to characterize the raw and activated materials but also for following the structural evolution during the first few hours of polycondensation (a spectrum was acquired every 10 minutes during a 13-hour period).

The compressive strengths of the samples were tested with a LLOYD EZ20 universal testing machine with a crosshead speed of 0.5 mm/min. For every composition, the measurements were performed on five cylindrical (15 mm diameter and 30 mm height) samples aged 28 days. The average compressive strength was expressed in MPa and represents the average of the five measurements.

The particle size distributions of the samples were obtained with a laser particle size analyzer, Mastersizer 2000. The powders were suspended by an airflow (3 Bars) through a glass cell with parallel faces illuminated by a beam of laser light.

Table 1: Chemical data of COx argillite (weight %).

SiO_2	Al_2O_3	MnO	MgO	CaO	Na_2O	K_2O	TiO_2	Fe_2O_3	P_2O_5	S	LOI (1000 °C)
48.68	13.41	0.03	2.50	10.73	0.20	3.26	0.72	4.51	0.07	0.83	15.06

The nuclear magnetic resonance (NMR) measurements were performed at room temperature with a Bruker Avance 400 spectrometer. The analyses were conducted with 400 scans at 104.26 MHz for [27]Al.

## III. Results

(1) Raw materials

Different argillite samples, thermally treated or not, were investigated in this study. Table 2 lists the various physical, chemical and structural data about the argillite samples.

Table 2: Physicochemical and structural data of raw, calcined and flash argillite (M = Ca or Mg)

	Si/Al[8]	D_{50} (µm)[8]	Al[IV] (%)[8]	Free MO (%)	Amorphous phase (%)
Ar	3,63	17	30	0	34
Ac	3,63	160	94	68	60
Af	3,63	21	68	13	46

The Si/Al ratio, the percentage of the Al[IV] content determined from ^{27}Al MAS-NMR and the particle size were issued from a previous study [8]. Previous studies have demonstrated that furnace calcination (samples Ac) allows a more complete dehydroxylation of the clay minerals than does flash calcination. The percentages of amorphous phase (Table 2) agree with this finding. In fact, the amorphous phase content increases from 34 % to 46 % and 60 % for Ar, Af and Ac samples, respectively. To identify the different weight losses, the mass spectrometry coupled with thermal analysis curves (Fig. 1) that correspond to the Ar, Ac and Af samples are presented. The mass/charge ratios (m/z) of 18, 44 and 64 are selected, since they correspond to the release of H_2O, CO_2 and SO_2, respectively, as previously identified by thermal analysis [8]. The various notable outgassed molecules are related to several reactions occurring at various temperatures (H_2O from the departure of physisorbed water, CO_2 due to the decomposition of carbonate species and SO_2 from sulfate compounds). More precisely, for raw argillite (Ar sample, Fig. 1a), the first H_2O contribution with a high intensity was observed between 25 and 225 °C, which corresponds to the release of physisorbed water. At temperatures between 500 and 800 °C, the second large H_2O contribution with a smaller intensity is related to water departure from various clay minerals or from dihydroxylation [15]. Contributions linked to an m/z of 44 with a lower intensity at temperatures between 650 and 800 °C correspond to the release of CO_2 resulting from the decomposition of the carbonate species (calcite and dolomite) [15, 16]. Furthermore, the SO_2 contributions (m/z = 44) were detected at 400 °C and 1100 °C and are related to the presence of a sulfur compound. The first release of sulfate (400 °C) is related to the presence of pyrite [17]. Lastly, the release of sulfur dioxide at approximately 1100 °C is related to cal-

cium sulfate decomposition [18, 19]. Calcium sulfate may be originally present in argillite and/or formed due to an *in-situ* reaction following the decomposition of carbonate compounds and the transformation of pyrite.

(a)

(b)

(c)
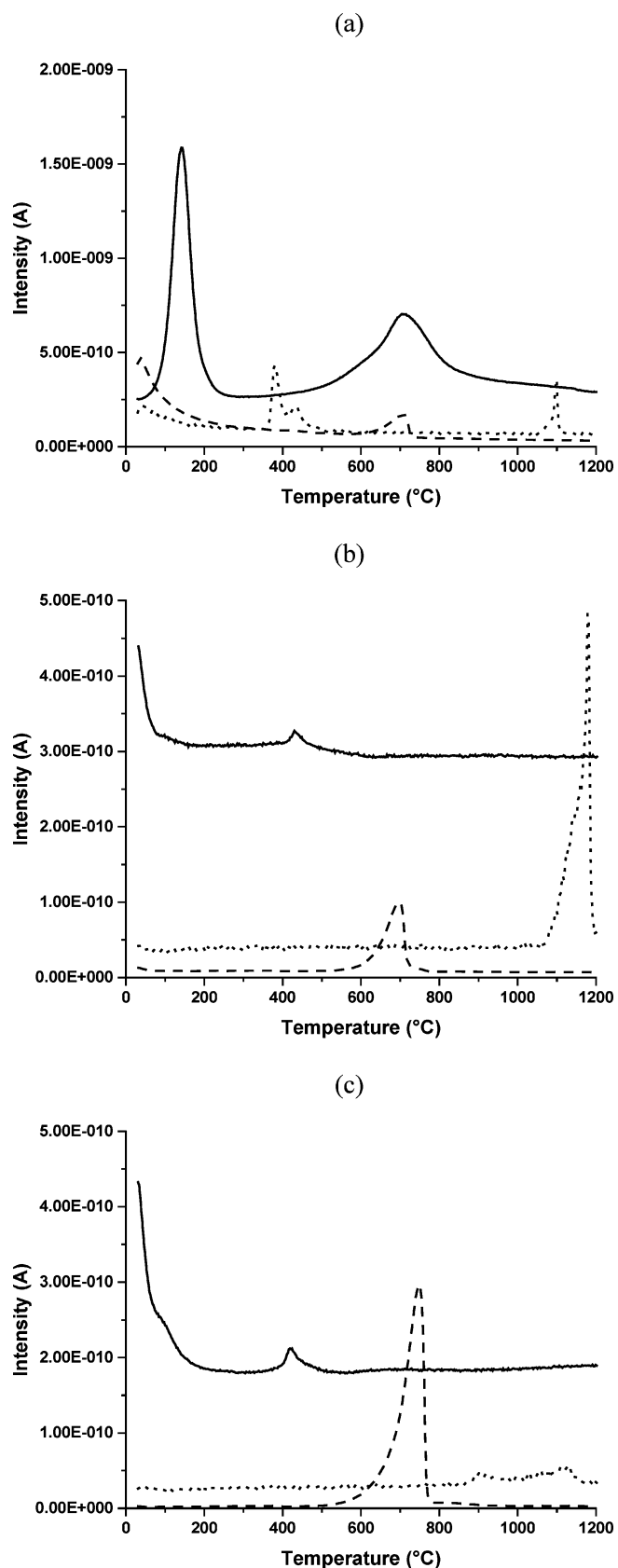
Fig. 1: Intensity of H_2O - m/z = 18 (–), CO_2 - m/z = 44 (---) and $SO_2 \times 10^2$ - m/z = 64 (⋯) as the function of the temperature get by thermal analysis coupled with mass spectrometer for (a) Ar, (b) Ac and (c) Af samples.

No matter what the thermal treatment of argillite is (Ac and Af samples, Fig. 1b and c, respectively), the H_2O contribution at approximately 500 – 800 °C disappears. However, a small contribution at a temperature less than 200 °C remains in the case of the Af sample and can be attributed to a hydrated compound (Mg or Ca based) or illite [15, 17, 18]. New contributions appear at temperatures of 390 and 410 °C for the Ac and Af samples, respectively. These contributions can be related to the $Mg(OH)_2$ transformation in the Af sample and $Ca(OH)_2$ decomposition in the Ac sample [15]. These data are in accordance with the different steps of dolomite decomposition previously observed [15, 16]. The contribution related to the carbon dioxide outgassing is always present at approximately 700 °C with various intensities and is characteristic of a carbonate species (calcite and dolomite), which is not completely decomposed. The Af sample presents a larger CO_2 contribution than does the Ac sample, which is greater in the presence of more available carbonates. For Af, an additional loss of SO_2 occurs at approximately 900 °C and is related to the outgassing of magnesium sulfate due to the solid-gas reaction between the magnesium, resulting from dolomite decomposition, and sulfate, resulting from pyrite decomposition [20, 21]. These data underscore the difference between the Af and Ac samples, notably in terms of the presence of the free alkaline earth cation (free lime and magnesia). To complete these data, the free alkaline earth compounds (Ca, Mg) were evaluated by thermal analysis (supplementary file) before and after calcination (Table 2). The value of 68 % for the Ac sample corresponds to the amount of the free alkaline earth cation divided by the total amount of M (Ca and Mg). This value, greater than that of the Af sample (13 %), is related to a high rate of decomposition for the carbonate species with a furnace treatment.

All these data highlight differences between the raw and calcined argillite samples with the various processes, especially in terms of the rate of dehydroxylation of the clay minerals and the presence of free alkaline earth cations dispensed from the carbonate species, suggesting a different reactivity for alkali activation.

(2)   *Alkali-activated materials based on COx argillite*

(a)   *Feasibility*

The feasibility of alkali-activated materials based on argillite was studied by the synthesis of several samples containing Ar, Ac and Af. The existence domains in an Ar-Ac-Af ternary diagram (Fig. 2) according to the weight percent of each argillite present in the sample were investigated. The feasibility is evaluated according to general characteristics, consolidation and water resistance. First, using pure Ac and Af argillites, the feasibility of the alkali-activated materials is optimal. However, for the Ar-based samples, there is no consolidation. Consequently, in the binary Ac-Af samples, consolidated materials are obtained, independent of the amount of Ac or Af used. In the Ac or Af samples with Ar, a limit of approximately 75 % of substitution is reached. In the following sections, six samples named A, B, C, D, E and F were selected to investigate their properties.
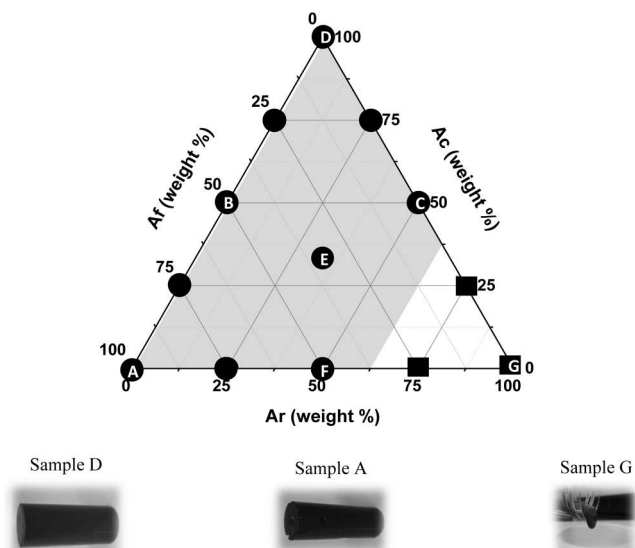

Fig. 2: Feasibility domains of Ar-Ac-Af alkali-activated materiel at room temperature: sufficient consolidation •, limited shaping ■.

(b)   *Structural evolution during formation*

The local structural formations were followed by *in-situ* FTIR measurements. Three examples of the obtained spectra at the initial and final time of the measurement for the GAf, $GAf_{0.5}Ac_{0.5}$ and $GAr_{0.5}Ac_{0.5}$ samples are given in Fig. 3A. For the GAf sample, at the beginning of the reaction (t = 0 min), the large peak at 3400 cm^{-1} is associated with -OH stretching, and a sharper peak centered at 1630 cm^{-1} is related to -OH bending of a water molecule [22]. Small shoulders at 2980 and 2940 cm^{-1} correspond to τ-CH (from hydrogen carbonate) [23]. Additionally, contributions of the carbonate species are visible at approximately 1550 – 1450 cm^{-1} [24]. The intense and large peak at approximately 1000 cm^{-1} corresponds to Si-O-M bonds (M = Si, Al, etc.) [25]. During the first 13 hours of the reaction, several modifications occur. The intensity of the water contribution decreases, and the intensity of the carbonate species increases slightly as well as their bond positions. The Si-O-M bond also shifts to a lower wavenumber. The spectra of the $GAf_{0.5}Ac_{0.5}$ and $GAr_{0.5}Ac_{0.5}$ samples present similar curves at the initial and final times, but the intensity of the carbonate and the Si-O-M bond position shifts are not the same. This shift is related to the transformation of the Si-O-Si bonds. Indeed, alkali activation leads to a substitution of the silicon by aluminum in the silicate network to form a 3D network of the geopolymer materials. This network results in the formation of Si-O-Al bonds and a shift in the Si-O-M bonds, which is characteristic of a polycondensation reaction [26]. The evolution of the carbonate contributions will be discussed in section III(3).

To correlate the FTIR shift with the kinetics of the reaction, Fig. 3B displays the shift in the Si-O-M bonds for the six studied samples according to the slope value. This slope value corresponds to the kinetics of the FTIR shift during the first 13 hours of the polycondensation reaction, i.e., 13 hours after the preparation of the reactive mixture. Two behaviors are distinguished: on one hand, the GAc (D), GAf (A) and $GAf_{0.5}Ac_{0.5}$ (B) samples are characterized by high shift and slope values
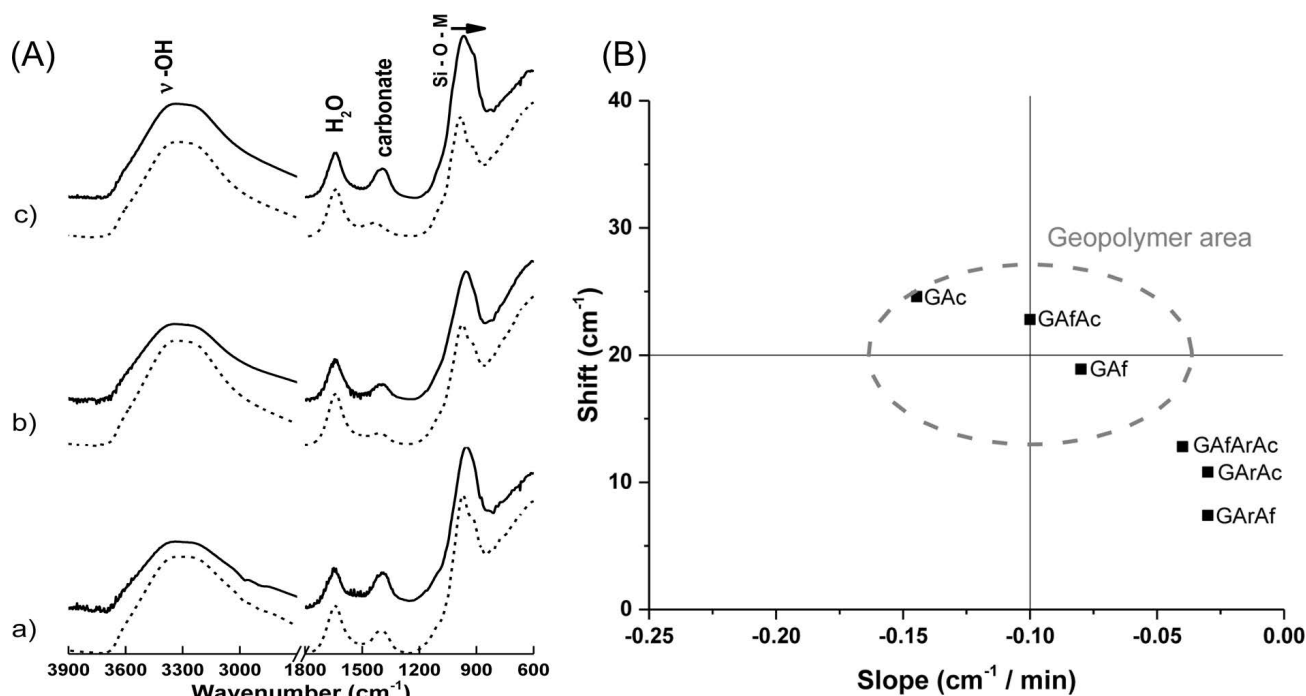
Fig. 3: (A) FTIR spectra of following in-situ measurement at initial time (---) and final time (–) for (a) GAf, (b) $GAf_{0.5}Ac_{0.5}$ and (c) $GAr_{0.5}Ac_{0.5}$ samples and (B) shift (Si-O-M) band value in function of the slope for the six samples.

(approximately 20 cm^{-1} and -0.10 cm^{-1}/min respectively); on the other hand, $GAf_{0.33}Ar_{0.33}Ac_{0.33}$ (E), $GAr_{0.5}Af_{0.5}$ (F) and $GAr_{0.5}Ac_{0.5}$ (C) exhibit lower shift and slope values (approximately 10 cm^{-1} and - 0.03 cm^{-1}/min respectively). Previously, A. Gharzouni *et al.* [27] defined an area of geopolymerization around a shift of 20 cm^{-1} and a slope of -0.10 cm^{-1}/min. According to these criteria, only the first group of samples, i.e. without Ar, leads to a polycondensation reaction. In the other samples, only a partial polycondensation reaction occurs. It is also notable that an increase in the calcined argillite proportion in the mixture increases the shift and the slope values favoring the geopolymerization reaction. Moreover, the increase in the proportion of raw argillite (Ar) in the mixture leads to a decrease in the shift and slope values. This fact can be explained by the higher reactivity of calcined argillite compared to raw argillite. Indeed, calcination allows the dehydroxylation of the clay minerals (kaolinite, illite, smectite, etc.), inducing an increase in the amorphous phase, which will be reactive in presence of an alkaline solution. This result agrees with the literature [8]. Indeed, it has been demonstrated that an improved reactivity is obtained by using a calcined clay at 750 °C.

The different behaviors observed during formation according to the used argillite samples suggest different structures and properties of the final alkali-activated materials.

(c) *Structural and mechanical properties of the alkali-activated materials*

To compare the structure of the different synthesized samples, X-ray diffraction was performed. Fig. 4A. displays three example X-ray patterns of the different alkali-activated samples after seven days and the Ac, Af and Ar raw materials. Compared to the Af raw material, the GAf

sample shows the presence of an amorphous dome centered at approximately 29 ° (2θ), demonstrating the polycondensation reaction observed for the geopolymer materials [28]. The diffraction peaks of illite/muscovite, quartz, calcite and dolomite present in the Af sample persist in the GAf alkali-activated material. Furthermore, the peaks that correspond to lime (i.e., the lime peaks) disappear. Additionally, for $GAf_{0.5}Af_{0.5}$, an amorphous dome is exhibited, and the lime peaks, initially observed in the Af and Ac raw materials, disappear. However, the carbonate peaks are well defined, which may be because the carbonates were not fully decomposed from the Af raw materials or new carbonates were formed during the alkali activation. The X-ray pattern of the $GAr_{0.5}Ac_{0.5}$ sample also shows an amorphous dome. The peaks attributed to lime disappear, and the pyrite and kaolinite peak intensities from the Ar raw materials are slightly discernible. To sum up, whatever the sample, alkali activation leads to the formation of an amorphous structure and the persistence of the crystalline phases initially present in the raw material(s) with the exception of lime for the Ac and Af-based samples [29]. The amorphous content strongly depend on the used argillite. An increase in the content of furnace-calcined and/or flash-calcined argillite favors the reaction and leads to the formation of a greater amorphous phase. This fact can be explained by the higher content of reactive aluminate and silicate in the calcined argillite (greater amorphous phase, Table 2) than in the non-calcined argillite. Moreover, the evolution of the carbonate species is different depending on the type and proportion of argillite.

More structural information was given by the FTIR measurements. The FTIR spectra of the argillite raw samples and alkali-activated materials aged seven days are presented in Fig. 4B. The summary of the positions and the assignment of the different contributions are provided in Table 3.

Compared to the Af sample, the GAf spectrum shows the disappearance of the νAl-OH of the illite, smectite and interlayered material initially detected at 3643 cm^{-1} [30, 31]. Moreover, a larger band at 3420 cm^{-1} of -OH stretching contribution is observed [22]. Concerning the carbonate species, a large band at approximately 1450 cm^{-1}, which is the result of the overlapping of several contributions from different carbonates, such as dolomite and calcite, is observed in the Af sample [24, 32]. After alkali activation (GAf), the intensities of dolomite and calcite located at approximately 1510 cm^{-1} decreased because of a new contribution link to the mixed carbonate species, which will be developed in section III(3)(b). The Si-O-Si bond initially located at 1028 cm^{-1} in the Af raw material shifts to 950 cm^{-1} [8, 33] and a new peak appears at approximately 930 cm^{-1}, related to Si-O-Ca formation [34]. The formation of GAf$_{0.5}$Ac$_{0.5}$ leads to the same transformation compared with that of GAf: i.e., an increase in the water contribution, the formation of a new carbonate species and a shift of Si-O-M to 943 cm^{-1}. Finally, GAr$_{0.5}$Ac$_{0.5}$ evolves similarly to the other samples. It is noticeable that the clay mineral initially present in the Ar sample (Al-OH stretching and

bending modes at 3698 and 913 cm^{-1}, respectively) is not detectable on the spectrum after alkali activation [8].

The structural differences between the synthesized samples are directly linked to the used raw materials and their reactivity induced by thermal treatment. The observed differences will impact the mechanical properties of the resulting materials.

(d) *Mechanical properties*

The mechanical properties of the different samples were evaluated by compressive strength measurements after 28 days of consolidation. To correlate the mechanical properties with the *in-situ* FTIR measurements, the evolution of the compressive strength and the FTIR shift in the Si-O-M peak position were plotted as a function of the Al concentration (calculated with the amount of aluminum and the volume of reactive mixture), as shown in Fig. 5. It is observed that the shift and the compressive strength values increase with an increase in the Al concentration. The samples containing non-calcined argillite, GAr$_{0.5}$Ac$_{0.5}$, GAr$_{0.5}$Af$_{0.5}$ and GAf$_{0.33}$Ar$_{0.33}$Ac$_{0.33}$

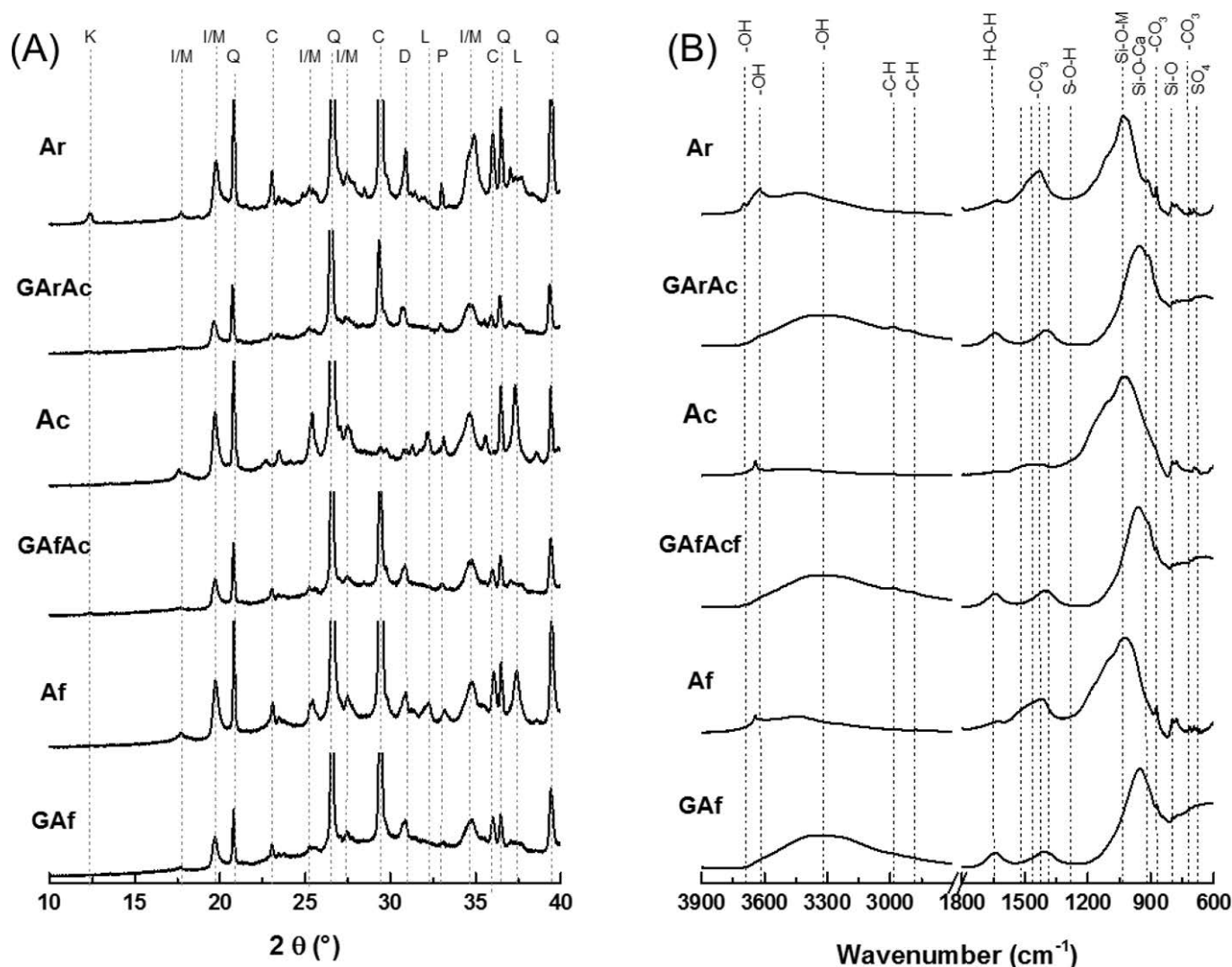**Fig. 4:** (A) XRD pattern and (B) FTIR spectrum of GAf, Af, GAf$_{0.5}$Ac$_{0.5}$, Ac, GAr$_{0.5}$Ac$_{0.5}$ and Ar samples. JCPDS files: K: kaolinite (00 – 001 – 0527), I/M: Illite/muscovite (04 – 019 – 1573), Q: quartz (04 – 016 – 2085), C: calcite (04 – 012 – 0489), D: dolomite (04 – 011 – 9833), L: lime (04 – 002 – 6758) and P: pyrite (04 – 011 – 7328).

Table 3: Assignment of FTIR contribution in argillites and alkali-activated samples.

Wavenumber (cm^{-1})	Attribution	Mineral	Bibliography
3696	ν OH	Kaolinite	[30]
3640–3620	ν O-H	Illite, smectite, interstratified	[31]
3400	ν H-O-H	H-bonded water	[22]
2977, 2939	ν C-H	C-H bands	[23]
1630	δ OH	Water of crystallization	[22]
1510	ν CO_3	Calcite	[32]
1454	ν CO_3	Dolomite	[24]
1432	ν CO_3	Calcite	[24]
1378	ν CO_3	K_2CO_3	[37]
1160	ν SO_4	Sulfites	[40]
1033	ν Si-O-Si	Clay mineral	[33]
930	ν Si-O-Ca	Calcium silicate	[34]
910	δ Al-O	Kaolinite	[8]
870	δ CO_3	Calcite	[23]
796, 774	δ Si-O	Quartz	[33]
691	δ Si-O	Quartz	[33]
613	δ -SO_4	Calcium sulfate	[40]

present the lowest compressive strengths (2, 2 and 8 MPa, respectively) and the lowest shift values, which correspond to the lowest aluminum concentration (~4 mol/L). The aluminum content does not appear sufficient in this case to promote a sufficient polycondensation reaction. As previously demonstrated in section III(2)(b), the $GAr_{0.5}Ac_{0.5}$, $GAr_{0.5}Af_{0.5}$ and $GAf_{0.33}Ar_{0.33}Ac_{0.33}$ samples did not facilitate the formation of a geopolymer network. For the calcined argillite-based samples, GAc, GAf and $GAf_{0.5}Ac_{0.5}$, the compressive strength values and shift values increase to 16 MPa and 20 cm^{-1}, respectively, with an increase in the Al concentration (up to 7.4 mol/L). Indeed, these samples present a higher rate of the reactive phase, which favors the polycondensation and geopolymerization reactions leading to stronger structure and hence better compressive strength [26]. This difference in the reactive phase is directly linked to the proportion of calcined argillite in the mixture. In fact, an increase in Ac and/or Af leads to an increase in aluminum concentration and thus improves the reactivity of the mixture. The differences in the mechanical strengths can also be linked to the difference in carbonate species evolution after alkali activation, and this hypothesis needs to be confirmed.

(3) Study of the carbonate species

(a) Thermal behavior

To understand the thermal behavior of the alkali-activated samples and the evolution of the carbonate species, the weight losses of the different samples were studied by TGA analysis. Fig. 6A, presents three examples of the
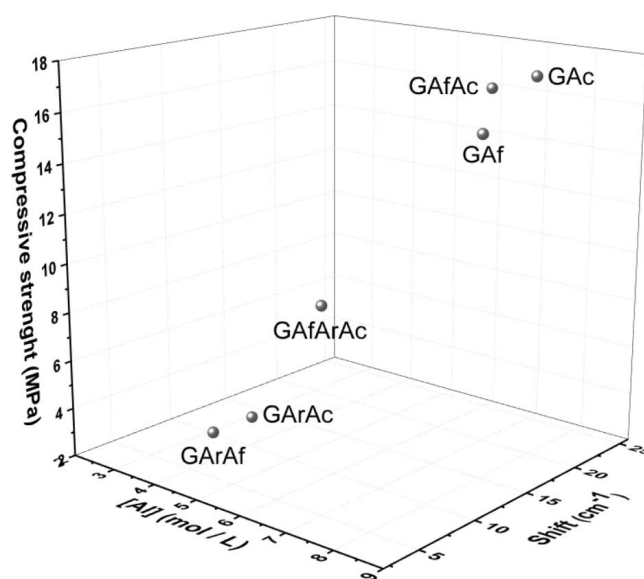
Fig. 5: Compressive strength (after 28 days) and FTIR shift of Si-O-M band values in function of the Al concentration for GAc, GAf, $GAf_{0.5}Ac_{0.5}$, $GAr_{0.5}Ac_{0.5}$, $GAr_{0.5}Af_{0.5}$ and $GAf_{0.33}Ar_{0.33}Ac_{0.33}$ alkali-activated samples.

TGA curves for GAf, $GAf_{0.5}Ac_{0.5}$ and $GAr_{0.5}Ac_{0.5}$ samples after seven days. Independent of the sample type, the first weight loss of 25 % occurs at a temperature lower than 600 °C (I), which corresponds mostly to physisorbed water and structural water due to the geopolymer network that decomposed before 200 °C. Moreover, between 200 and 600 °C, there is a water loss due to the hydroxyl groups in the clay minerals (mainly in Ar). Two additional weight losses occur between 620 and 680 °C (II) and after 750 °C (III), which are related to carbonate species decomposition

and CO_2 formation [14, 15]. Differences can be detected between the different samples. The three weight losses of all the alkali-activated samples are presented in Fig. 6B. The first weight losses (I) are between 25 and 30 %, which is in accordance with the values commonly obtained for alkali-activated binders [25]. Lower weight loss values (~ 26 %) are obtained for samples based only on calcined argillite, which suggests a better geopolymer network. This result is in accordance with section III(2)(d) that shows a higher compressive strength in the case of these samples [26, 35].

(A)

(B)

Fig. 6: (A) Example of thermal analysis curves for GAf (–), $GAf_{0.5}Ac_{0.5}$ (---) and $GAr_{0.5}Ac_{0.5}$ (...) samples after seven days and (B) weight losses for all alkali-activated samples at seven days.

The first CO_2 loss that occurs between 600 and 750 °C (II) is probably related to mixed carbonate species or carbonate compounds based on an alkaline earth cation. The minimal value, close to zero, is observed for the GAc sample. Samples based on a mixture of Ac and Af/Ar present intermediate losses, of approximately 2 %, and a loss of 3 % is demonstrated by the $GAf_{0.33}Ar_{0.33}Ac_{0.33}$ sample. The most important losses, approximately 4 %, are relat-

ed to samples without Ac. Indeed, Ac is quasi-totally decarbonated, and consequently, there is no CO_2 to release. Af and Ar exhibits a high content of carbonate, and, after alkali activation, the same weight loss occurs.

The final weight loss, above 750 °C (III), is linked to the decomposition of the most refractory carbonate, namely, calcite. The losses are very small (~ 0.2 %) for samples based on calcined argillite (using both furnace and flash treatment processes). With the presence of Ar, this loss slightly increases (~ 0.6 %).

At temperatures above 800 °C (data not shown), the low weight loss (approximately 1 %) is due to the formation of SO_2 issued from K_2SO_4, which suggests a reaction between potassium and sulfur [36].

To correlate the different losses to the decomposition of the carbonate species, Fig. 7 displays the evolution of the molar percentage of CO_2 released during the TGA measurement as a function of the molar percentage of the free alkaline earth cation in the sample. Initially, for temperature between 600 and 750 °C, the GAc sample presents the smallest CO_2 loss (~ 1 %), and the GAf sample presents the highest loss (~ 7.5 %). Indeed, in the Ac argillite sample, the carbonate species are mostly decomposed, whereas in Af a higher release rate of the carbonate species is exhibited because the carbonate species did not fully decompose. The loss obtained with $GAf_{0.5}Ac_{0.5}$ (~ 4 %) is between that of the GAf and GAc samples, which suggests a proportionate release of CO_2 and free M^{2+}. The addition of Ar argillite in GAc formed $GAr_{0.5}Ac_{0.5}$, which led to a decrease in the free M^{2+} amount (until 3.5 %) and then an increase in CO_2 formation (~ 4 %), which confirms this proportionality. The $GAr_{0.5}Af_{0.5}$ sample shows the same CO_2 loss compared with that of GAf (7.5 %) but a lower M^{2+} content (0.5 %), probably linked to the high amount of carbonate species in both Ar and Af argillite. Lastly, the $GAf_{0.33}Ar_{0.33}Ac_{0.33}$ sample presents approximately 3 % free M^{2+} and a CO_2 loss close to 6 %, which confirms the linear relation between M^{2+} and the first CO_2 loss.

Fig. 7: Evolution of the molar percent of CO_2 release during thermal analysis between (■) 600 – 750 °C and (□) 750 – 800 °C according to the molar ratio of free M^{2+} cations (Ca, Mg) in the alkali-activated samples GAf, $GAf_{0.5}Ac_{0.5}$, $GAr_{0.5}Ac_{0.5}$, GAc, $GAf_{0.33}Ar_{0.33}Ac_{0.33}$ and $GAr_{0.5}Af_{0.5}$ samples after seven days.

For the second loss between temperatures of 750 and 800 °C, which corresponds to the decomposition of other types of carbonates, small variations are observed between the samples. GAf, $GAf_{0.5}Ac_{0.5}$ and GAf present similar CO_2 losses under 0.5 %. The addition of Ar argillite leads to a small increase in this loss, up to 1.3 %, for the $GAr_{0.5}Ac_{0.5}$, $GAr_{0.5}Ac_{0.5}$ and $GAf_{0.33}Ar_{0.33}Ac_{0.33}$ samples. These data confirm that this second loss is not related to the M^{2+} content, but to carbonate that is not decomposed with a thermal treatment at 750 °C.

The thermal analysis highlights different types of carbonates, which originate from the used raw materials or newly formed after alkali activation, but did not precisely identify them. Structural analyses using FTIR spectroscopy and XRD will be useful in this case.

(b) *Evolution of the carbonate species*

To identify the carbonate species in argillite according to different thermal treatments, and their evolution with alkali activation, a focused study on the carbonate contribution using FTIR spectroscopy and X-ray diffraction was performed (Fig. 8). Fig. 8A represents the FTIR spectra of the argillite (Ar, Af, Ac) and alkali-activated samples after seven days.

Compared to Af argillite, the GAf sample shows the appearance of a new band between 1415 and 1380 cm^{-1} related to the formation of a mixed carbonate (with alkali and alkaline earth cations) due to alkali activation [37]. Moreover, the contribution of dolomite (1455 cm^{-1}) and calcite at a higher wavenumber (1510 cm^{-1}) disappears [21, 31].

The same evolution is observed in the $GAf_{0.5}Ac_{0.5}$ sample with a decrease in the intensity due to the low amount of carbonate species in the Ac sample. For the GAc sample, the intensity of the carbonate contributions strongly decreases for the same reason. Indeed, the Ac spectrum displays a very low intensity for all the carbonate bands, and no contribution related to mixed carbonates is exhibited. Then, the progression of the $GAr_{0.5}Ac_{0.5}$ sample is similar to the other alkali-activated samples with the formation of the mixed carbonates. The same behavior is observed with $GAf_{0.5}Ar_{0.5}$ in contrast to raw argillite, Ar, in which there is no indication of a mixed carbonate formation; but clear contributions from calcite (1510 and 1430 cm^{-1}) and dolomite (1455 cm^{-1}) are present. Finally, the $GAf_{0.33}Ar_{0.33}Ac_{0.33}$ sample presents only calcite and mixed carbonate contributions due to the alkali activation of the argillites. The presence of potassium issues from the silicate solution in excess, leading to carbonate mixed compounds or to the formation of K_2SO_4 [36].

To improve the identification of carbonate species, measurement with Raman spectroscopy has been performed but the spectra cannot be used because of the fluorescence due to the iron in the argillite. Therefore, X-ray diffraction is used to complete the FTIR analysis.

Fig. 8B shows the X-ray patterns of the argillite samples (Ar, Af and Ac) and of the alkali-activated samples after seven days. Only the $28-33$ ° (2θ) range is presented in order to focus on carbonate species and sulfates. Two different large contributions can be distinguished: at approximately 29.5 ° (2θ) that correspond to the
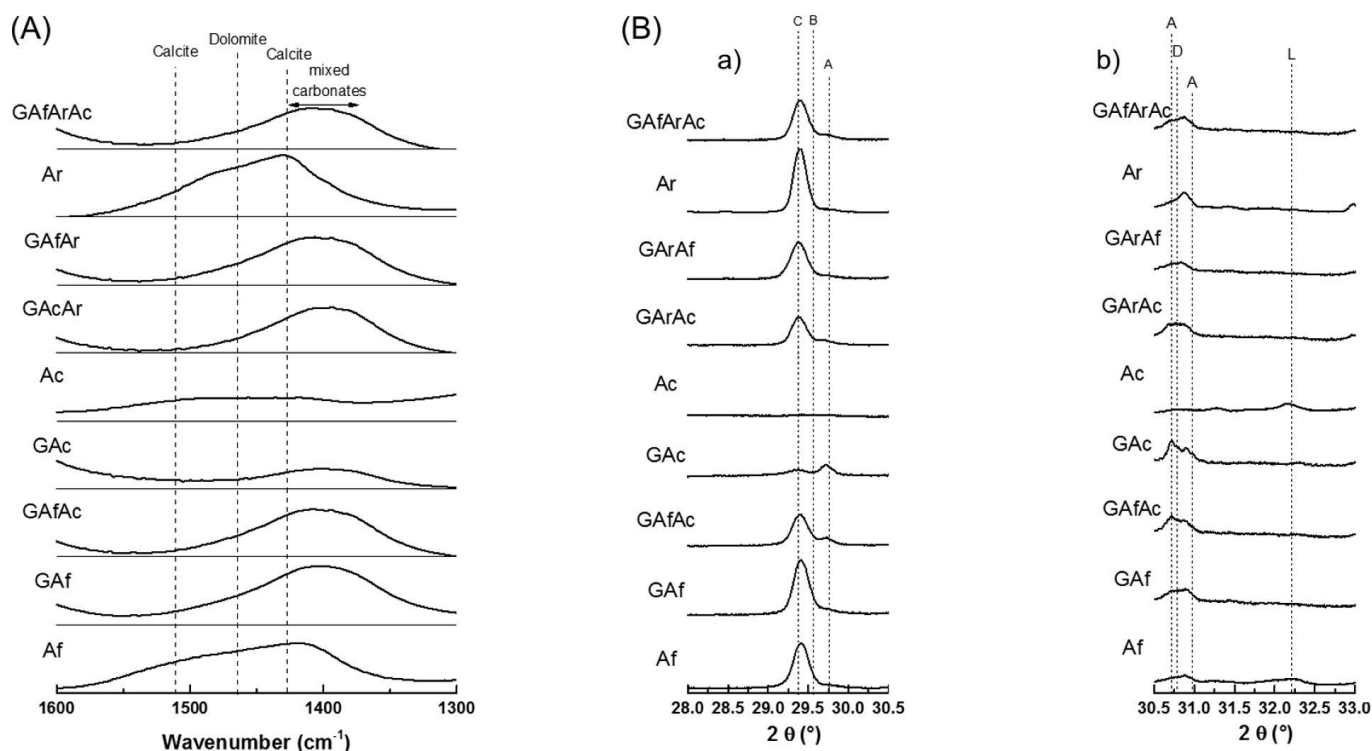
Fig. 8: (A) FTIR spectra and (B) X-ray patterns focus on the carbonate species ($28-30.5$° (a) and $30.5-33$° (b) ranges with different scale) for raw materials (Ac, Af and Ar) and alkali activated samples after seven days (GAf $GAf_{0.5}Ac_{0.5}$, GAc, $GAr_{0.5}Ac_{0.5}$, $GAr_{0.5}Af_{0.5}$ and $GAf_{0.33}Ar_{0.33}Ac_{0.33}$). JCPDS files: C: $CaCO_3$ ($04-012-0489$), B: $K_2Ca(CO_3)_2$ ($00-025-0626$), A: K_2SO_4 ($04-006-8317$), D: $CaMg(CO_3)_2$ ($04-011-9833$) and L: CaO ($04-002-6758$).

carbonate species (Fig. 8 B (a)) and close to 31° (2θ) due to the carbonate species and sulfate contributions (Fig. 8 B (b)). These diffraction lines are wide, and their angular ranges are evolving according to the nature of the sample, suggesting different reactions. For the first peak, different possible contributions have been identified as calcite ($CaCO_3$), butschliite ($K_2Ca(CO_3)_2$) and arcanite (K_2SO_4). For the second peak, the middle contribution is identified as dolomite ($CaMg(CO_3)_2$) and is surrounded by two contributions of arcanite. Finally, for the raw materials, Af and Ac, another peak can be seen at approximately 32° (2θ) associated with lime.

Compared to the Af sample, GAf does not show a peak that corresponds to lime, which disappears with alkali activation. Additionally, an arcanite peak appears at 31° (2θ), which is possibly due to an excess of potassium from the alkali-silicated solution. Moreover, the peak of calcite shifted to a higher angle, probably due to the appearance of new mixed carbonate species (butschliite). The $GAf_{0.5}Ac_{0.5}$ sample presents a smaller peak at 29.5° (2θ) due to the lower amount of carbonate species in Ac, and there is also an increase in intensity in the arcanite peak. This behavior is confirmed for the GAc sample, which barely presents the carbonate species and arcanite peaks. Indeed, argillite Ac does not show either a carbonate or sulfate peak but does exhibit a well-defined lime peak at 32.5° (2θ). The $GAr_{0.5}Ac_{0.5}$ sample confirms the disappearance of the lime peak and the formation of arcanite, which is consistent with the alkali activation and the modification of the large carbonate peak including calcite and mixed carbonate species. With Af argillite, the $GAr_{0.5}Af_{0.5}$ sample presents the same XRD pattern, but the arcanite peaks are less discernible. Finally, for the $GAf_{0.33}Ar_{0.33}Ac_{0.33}$ sample, there is again a shift and a widening of the calcite peak, which signifies a new carbonate species and the formation of arcanite.

The results indicate that the alkali activation of calcined argillite (or mixture of raw and calcined argillite) leads to the formation of new mixed carbonates based on potassium. Indeed, there are unstable alkali earth cations resulting from the decomposition of the carbonate species during various thermal treatments [8]. Moreover, the high concentration of the alkaline silicate solution probably led to an excess of potassium in the mixture that can react with the carbonate formed by the alkali earth cations and form arcanite. The findings suggest that this sulfate formed during alkali activation with a high potassium concentration and the pyrite decomposition products.

IV. Discussion

All the previous data highlight the structural differences between the synthesized samples. These differences are strongly related to the thermal treatment of the argillite samples that influence essentially the aluminum and alkaline earth cations in the mixture. For this, correlations were established in Fig. 9 between the reactive Al, the free alkaline earth cations and the FTIR shift in the Si-O-M band of the different studied samples. The reactive aluminum was calculated by the amount of Al^{IV} (determined by NMR) multiplied by the amorphous rate, and then this quantity was divided by the amount of Al^{VI} (Table 2).
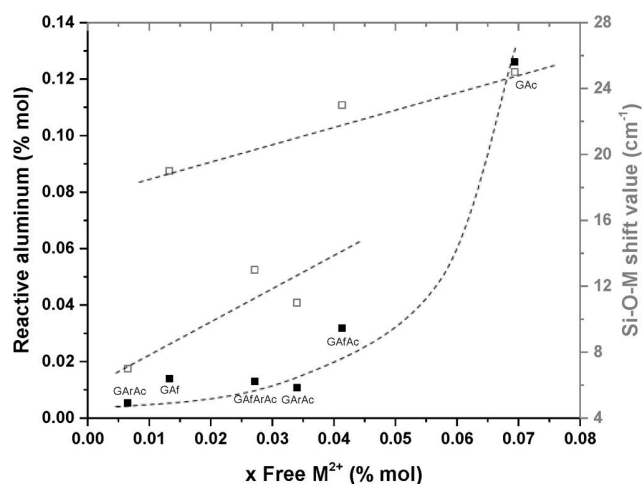

Fig. 9: (■) Rate of reactive aluminum and (□) FTIR shift of the Si-O-M bonds according to the molar percent of free M^{2+} cations (Ca or Mg) in the different samples GAf, $GAf_{0.5}Ac_{0.5}$, $GAr_{0.5}Ac_{0.5}$, GAc, $GAf_{0.33}Ar_{0.33}Ac_{0.33}$ and $GAr_{0.5}Af_{0.5}$ samples after seven days.

On one hand, the increase in the proportion of calcined argillite (with flash and, to a greater degree, with furnace calcination) leads to an increase in the amounts of reactive aluminum from 2 to 12 % and free lime from 0.5 to 7 % for the $GAr_{0.5}Af_{0.5}$ and GAc samples, respectively. This result can be explained by the higher degree of dehydroxylation of the clay minerals using furnace calcination of the Ac sample compared with using flash calcination of the Af sample and non-treated argillite (Ar). Therefore, more aluminum is released from the aluminosilicate source, which enables a polycondensation reaction. Moreover, the degree of carbonate decomposition is also higher using furnace calcination (Ac sample) compared to the decomposition using flash calcination (Af sample and the non-treated argillite (Ar)), inducing more free alkaline earth cations in the mixture.

On the other hand, the FTIR shift increases from 6 to 24 cm^{-1} with an increase in the amount of free M^{2+} from 0.5 to 7 % in $GAr_{0.5}Af_{0.5}$ and GAf. Once again, the importance of thermal treatment and its influence on the structural evolution of the samples is demonstrated. In fact, the two groups of samples can be distinguished: the samples containing raw argillite ($GAr_{0.5}Ac_{0.5}$, $GaR_{0.5}Af_{0.5}$ and $GAf_{0.33}Ar_{0.33}Ac_{0.33}$) exhibit a low amount of M^{2+} and smaller shift values; and the samples containing calcined argillite (the GAf, $GAf_{0.5}Ac_{0.5}$ and GAc samples) exhibit a higher quantity of M^{2+} and higher shift values. The increase in the shift value indicates the formation of a higher number of Si-O-Al bonds from the Si-O-Si bonds, which indicates the formation of an improved geopolymer network [26, 38, 39].

All the previous results prove the suitability of COx argillite after heat treatment to produce alkali-activated materials and aid in the understanding of the evolution of the different constituents of COx argillite after thermal treatment at 750 °C and alkali activation with a potassium alkaline solution, as summarized in Fig. 10:

- The thermal treatment allows the dehydroxylation of the clay minerals (illite, muscovite, smectite, chlorite, and kaolinite) present in COx argillite.
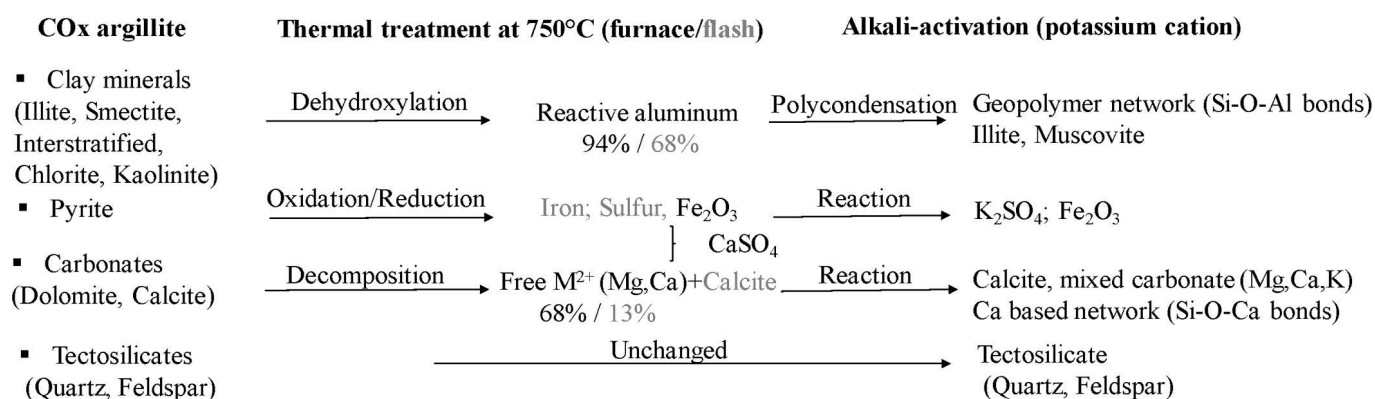
COx argillite	Thermal treatment at 750°C (furnace/flash)		Alkali-activation (potassium cation)
▪ Clay minerals (Illite, Smectite, Interstratified, Chlorite, Kaolinite)	→Dehydroxylation→	Reactive aluminum 94% / 68% →Polycondensation→	Geopolymer network (Si-O-Al bonds) Illite, Muscovite
▪ Pyrite	→Oxidation/Reduction→	Iron; Sulfur, Fe_2O_3 →Reaction→	K_2SO_4; Fe_2O_3
		} $CaSO_4$	
▪ Carbonates (Dolomite, Calcite)	→Decomposition→	Free M^{2+} (Mg,Ca)+Calcite 68% / 13% →Reaction→	Calcite, mixed carbonate (Mg,Ca,K) Ca based network (Si-O-Ca bonds)
▪ Tectosilicates (Quartz, Feldspar)	→Unchanged→		Tectosilicate (Quartz, Feldspar)

Fig. 10: Summary of the evolutions of the main mineral compounds in the argillite according to the thermal treatment and the alkali-activation.

The dehydroxylation is more complete with furnace calcination compared to flash calcination, leading to an increase in reactive aluminum in the mixture (the Al^{IV} percentages are approximately 68 % and 94 % for flash and furnace calcination, respectively). This reactive aluminum is essential for a polycondensation reaction and the formation of a geopolymer network (Si-O-Al bonds). Some illite and muscovite persist in the final material, which does not depend on the thermal treatment process.

- Whatever the process, thermal treatment induces the reduction of iron and the oxidation of sulfur in pyrite. In furnace-calcined argillite, the formation of hematite is responsible for the orange-reddish color. After alkali activation, the sulfate may interact with potassium to form potassium sulfate (K_2SO_4), which was more abundant in samples based on furnace-calcined argillite.
- In the case of the carbonates, which are essentially calcite and dolomite in COx argillite, their decomposition depends on the calcination temperature/duration and atmospheric conditions. Furnace thermal treatment induces the decomposition of carbonates producing free alkaline earth cations (especially free lime) (M^{2+}, 68 %). Some of the calcium can interact with sulfate resulting from pyrite oxidation to form $CaSO_4$. In the case of flash calcination, the decomposition is not complete, leading to a lower amount of free alkaline earth cations (M^{2+}, 13 %) and the persistence of some calcite. After alkali activation, several interactions occur between free cations to form mixed carbonates and calcite but also other calcium-based network (Si-O-Ca) bonds.
- The tectosilicate present in COx argillite, essentially quartz and feldspar, is resistant to thermal treatment and alkali activation and persists in the final structure.

V. Conclusions

To study a different method for the valorization of Callovo-Oxfordian (COx) argillite, alkali activation has been examined. After a previous study concerning the activation of COx argillite by a thermal treatment [8], this study aims to investigate the formation, structure and mechanical properties of the alkali-activated materials based on COx argillite. For this, the feasibility of consolidated materials containing raw, furnace- and flash-calcined argillite in presence of a potassium alkaline solution was evaluated. It was demonstrated that both furnace and flash treatments, and a mixture of raw and calcined argillite are suitable for the alkali activation of the consolidated samples. FTIR spectroscopy data demonstrate a polycondensation reaction and the formation of a geopolymer network in samples containing calcined argillite. However, the reaction is not favored in the sample containing non-treated argillite. This result agrees with compressive strength measurements, which are higher in samples based on calcined argillite (16 MPa). Thus, it was possible to determine the reactivity of argillite, heated or not, in presence of a potassium alkaline solution:

(i) The non-treated argillite exhibits a very low reactivity or is non-reactive in presence of the alkaline solution due to very small amount of aluminum, which can be dissolved, and the presence of crystalline phases. Therefore, aluminum can be used in alkali-activated materials only as a filler.

(ii) The reactivity of argillite increases with flash calcination at 750 °C due to the partially dehydroxylated clay minerals and decomposed carbonates leading to higher amount of reactive aluminum and free alkaline cations in the mixture. A polycondensation reaction was effective in leading to a relatively sufficient mechanical strength. The presence of free alkaline oxides leads to several interactions and the formation of new carbonates and other networks containing calcium. The remaining or newly formed carbonates do not perturb the reaction. This thermal treatment process seems beneficial from an ecological and economical point of view.

(iii) The furnace calcination of argillite at 750 °C is more efficient in terms of the dehydroxylation of clay minerals and decomposition of carbonates. The polycondensation reaction is favored, leading to good mechanical strength.

(iv) The mixture of flash- and furnace-calcined argillite exhibits a similar reaction rate and mechanical strength compared with furnace-calcined argillite.

(v) The presence of non-calcined argillite in the mixture slows down the polycondensation reaction and weakens the structure.

According to these results, a thermal treatment is essential to increase the chemical reactivity of argillite to develop alkali-activated materials. Therefore, it is possible to valorize COx argillite by using alkali-activation. Depend-

ing on the targeted applications in the Cigéo project and the requested working properties, the flash and/or furnace calcination processes can be varied.

VI. Appendix

Supplementing our results detailed under III. Results (1) Raw Materials, additional data are provided in the following.

Fig. 11 shows the DTA-DTG curves of raw argillite (Ar) and furnace-treated argillite at 750 °C (Ac).
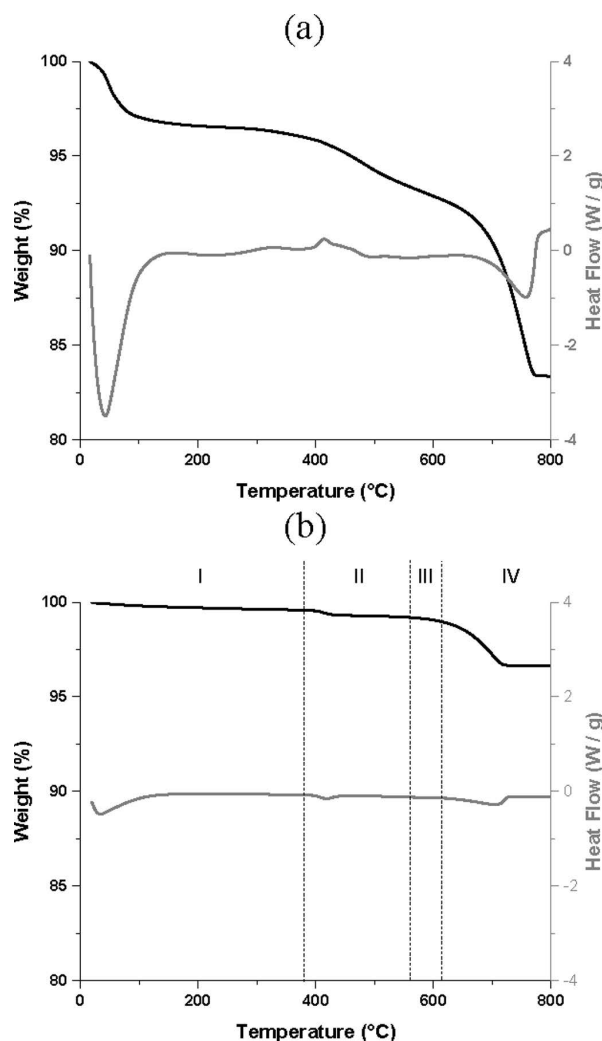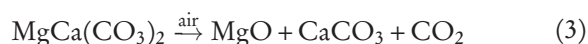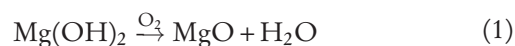

Fig. 11: DTA-DTG curve of (a) Ar and (b) Ac.

Thermal analysis of the raw argillite, Ar sample, (Fig. 11a) shows a weight loss of 15.33 % of CO_2, which is considered as the total decarbonation of argillite. This value is in accordance with the amount of CaO and MgO obtained with X-ray fluorescence analysis. The thermo-

gram of the calcined argillite, Ac sample, (Fig. 11b) displays four weight losses. The first one (I), between 25 and 375 °C, is related to the release of the structural water of the argillite. The second (II), between 375 and 550 °C, corresponds to water loss from the decomposition of the $Mg(OH)_2$ formed during the calcination (Eq. 1). The third loss (III), between 550 and 625 °C, is associated with a first decarbonation related to the calcite formed consecutively to the decomposition of the dolomite (Eq. 2, Eq. 3). Last, above 625 °C (IV) the second decarbonation (discernible by a heat flow variation) is related to the calcite decomposition (Eq. 2). Indeed, the calcite is naturally more stable in temperature than dolomite, which is confirmed by the weight loss (II).

$$Mg(OH)_2 \xrightarrow{O_2} MgO + H_2O \qquad (1)$$

$$CaCO_3 \xrightarrow{air} CaO + CO_2 \qquad (2)$$

$$MgCa(CO_3)_2 \xrightarrow{air} MgO + CaCO_3 + CO_2 \qquad (3)$$

Quantification of the free earth alkaline cations formed during the thermal treatment is performed with the TGA measurements coupled with a mass spectrometer. It appears that the dehydroxylation of clays minerals occurs mainly between 450 and 550 °C, so it was chosen to use the weight losses above 550 °C (and check that they really correspond to decarbonation processes). The different amounts of CO_2 (in molar percent) and water (from dihydroxylation) are compared to the value obtained by means of X-ray fluorescence and the Rietveld data. All these data are collected in Table 4.

The amount of water released during the second weight loss (II) for the samples Ac and Af corresponds to the amount of magnesium present in the dolomite, i.e. 1.6 % (TGA) and 1.8 % (Rietveld). These data confirm the identification of these losses and that the thermal treatment at 750 °C is sufficient to entirely decompose the dolomite.

The available calcium rate is calculated with the other weight losses and the amount of free alkali earth cation is estimated with Eq. 4.

$$\text{rate of free cation} = \frac{n\,CO_2^{1st\,loss} + (n\,CO_2^{2nd\,loss} - n\,CO_2^{Ar})}{n\,(Ca + Mg)^{total\,X\text{-}ray\,fluo}} \qquad (4)$$

The flash treatment at 750 °C, Af sample, leads to a rate of 12.8 % of free earth alkali cation, in accordance with the partial decomposition of the different carbonates species. The furnace treatment at 750 °C, Ac sample, leads to 68 % reactive M^{2+} cation. However, some carbonate species are not decomposed.

Table 4: Molar percent of H_2O and CO_2 obtain with TGA measurements

| Samples | Mg cation | Ca cation | | | Free % M^{2+} |
	x H_2O	I x CO_2	II x CO_2	Σ x CO_2	± 5
Ar	0	1,6	13,8	15,4	--
Af	1,6	2,2	14,2	16,4	12,8
Ac	1,6	1,3	3,2	4,5	68,3

References

[1] Andra: Folder clay 2005, Evaluation of the feasibility of a geological repository in an argillaceous formation. Andra, Châtenay-Malabry, France, 2005.

[2] Montes, H.G., Duplay, J., Martinez, L., Escoffier, S., Rousset, D.: Structural modification of callovo-oxfordian argillite under hydratation/dehydratation condition, *Appl. Clay Sci.*, **25**, 187–194, (2004).

[3] Glukhovsky, V.D.: Soil silicate based product and structures. Gosstroiizdat Publish, Kiev, URSS, 1957.

[4] Davidovits, J.: Geopolymer: chemistry and application. Institut Géopolymère, Saint-Quentin, France, 2008.

[5] Wan, Q., Rao, F., Song, S., Leon-Patiño C.A.: Geothermal clay-based geopolymer binders: synthesis and microstructural characterization, *Appl. Clay Sci.*, **146**, 223–229, (2017).

[6] Essaidi, N., Samet, B., Baklouti, S., Rossignol, S.: Feasibility of producing geopolymer from two different tunisian clay before and after calcination at various temperature, *Appl. Clay Sci.*, **88**, 221–227, (2014).

[7] Ogundiran, M.B., Kumar, S.: Synthesis and characterization geopolymer from nigerian clay, *Appl. Clay Sci.*, **108**, 173–181, (2015).

[8] Gharouni, A., Dupuy, C., Sobrados, I., Joussein, E., Texier-Mandoki, N., Bourbon, X., Rossignol, S.: The effect of furnace and flash heating on COx argillite for the synthesis of alkali-activated binders, *J. Clean. Prod.*, **156**, 670–678, (2017).

[9] Antoni, A., Wibiatma Wijaya, S., Satria, J., Surgiarto, A., Hardijito, D.: The use of borax in deterring flash setting of high calcium fly ash based geopolymer, *Mater. Sci. Forum*, **857**, 416–420, (2016).

[10] Phummiphan, I., Horpibulsuk, S.: High calcium fly ash geopolymer stabilized lateritic soil and granulated blast furnace slag bends as a pavement base material, *J. Hazard. Mater.*, **341**, 257–267, (2018).

[11] Yip, C.K., Lukey, G.C., Van Deventer, J.S.J.: The coexistence of geopolymeric gel and calcium silicate hydrate at the early stage of alkaline activation, *Cement Concrete Res.*, **35**, 1688–1697, (2005).

[12] Peyne, J., Gautron, J., Doudeau, J., Joussein, E., Rossignol, S.: Influence of calcium addition on calcined brick clay based geopolymers: a thermal and FTIR spectroscopy study, *Constr. Build. Mater.*, **152**, 794–803, (2017).

[13] Djobo, Y.J.N, Elimbi, A., Dika Manga, J., Djon Li Njock, I.B.: Partial replacement of volcanic ash by bauxite and calcined oyster shell in the synthesis of volcanic ash-based geopolymers, *Constr. Build. Mater.*, **113**, 673–681, (2016).

[14] Prud'homme, E., Michaud, P., Joussein, E., Clacens, J.M., Rossignol, S.: Role of alkaline cations and water content on geomaterial foams: monitoring during formation, *J. Non-Cryst. Solids,* **357**, 1270–1278, (2011).

[15] Foldvari, M.: Handbook of thermogravimetric system of minerals and its use in geological practice. Occasional Papers of the Geological Institute of Hungary, Budapest, Hungary, 2011.

[16] Olszak-Humienik, M., Jablonski, M.: Thermal behavior of natural dolomite, *J. Therm. Anal. Calorim.,* **119**, 2239–2248, (2015).

[17] Zhao, H., Bai, Z., Bai, J., Guo, Z, Kong, L., Li, W.: Effect of coal particle size on distribution and thermal behaviour of pyrite during pyrolysis, *Fuel*, **148**, 145–151, (2015).

[18] Engbrecht, D.C., Hirschfeld, D.A.: Thermal analysis of calcium sulfate dihydrate sources used to manufacture gypsum wallboard, *Thermochim. Acta*, **639**, 173–185, (2016).

[19] Higuchi, K., Gushima, A., Ikeda, T.: Synthesis of calcium ferrite from waste gypsum board, *ISIJ Int.*, **56**, 168–175, (2016).

[20] Sieranski, T., Kruszynski, R.: Magnesium sulphate complexes with hexa-methylenetetramine and 1,0-phenanthroline, *J. Therm. Anal. Calorim.*, **109**, 141–152, (2012).

[21] Gao, C., Li, X., Feng, L., Xiang, A., Zhang, D.: Preparation and thermal decomposition of 5 $Mg(OH)_2 \cdot MgSO_4 \cdot 2H_2O$ nanowhiskers, *Chem. Eng. J.*, **150**, 551–554, (2009).

[22] Socrates, G.: Infrared and Raman Characteristic group Frequencies, Tables and Charts. 3rd edition. John Wiley & Sons, Inc, New York, 2004.

[23] Schäfer, T., Michel, P., Claret, F., Wirick, S., Jacobsen, C.: Radiation sensitivity of natural organic matter: clay mineral association effects in the callovo-oxfordian argillite, *J. Electron Spectrosc.*, **170**, 49–56, (2009).

[24] Huang, C.K., Kerr, P.F.: Infrared study of the carbonate minerals, *Am. Mineral.*, **45**, 311–323, (1960).

[25] Ozer, I., Soyer-Uzun, S.: Relations between the structural characteristics and compressive strength in metakaolin based geopolymers with different molar Si/Al ratios, *Ceram. Int.*, **41**, 10192–10198, (2015)

[26] Gharzouni, A., Joussein, E., Samet, B., Baklouti, S., Rossignol, S.: Effect of the reactivity of alkaline solution and metakaolin on geopolymer formation, *J. Non-Cryst. Solids,* **410**, 127–134, (2015).

[27] Gharzouni, A., Sobrados, I., Joussein, E., Baklouti, S., Rossignol, S.: Predictive tools to control the structure and the properties of metakaolin based geopolymer materials, *Colloid. Surface. A*, **511**, 212–221, (2016).

[28] Prud'homme, E., Michaud, P., Joussein, E., Clacens, J.M., Rossignol, S.: Role of alkaline cation and water content on geomaterial foams: monitoring during formation, *J. Non-Cryst. Solids,* **357**, 270–1278, (2011).

[29] Autef, A., Prud'homme, E., Joussein, E., Gasgnier, G., Pronier, S., Rossignol, S.: Evidence of a gel in geopolymer compounds from pure metakaolin, *J. Sol-Gel Sci. Techn.*, **67**, 534–544, (2013).

[30] Joussein, E., Petit, S., Decarreau, A.: A new method to determine the ratio of clays minerals in mixtures by IR spectroscopy, *Earth Planet. Sc. Lett.*, **332**, 83–89, (2001).

[31] Srasra, A., Bergaya, F., Fripiat, J.J.: Infrared spectroscopy study of tetrahedral and octahedral substitutions in an inter-stratified illite-smectite clay, *Clay. Clay Miner.*, **42**, 237–241, (1994).

[32] Henry, D.G., Watson, J.S., John, C.M.: Assessing and calibrating the ATR-FTIR approach as a carbonate rock characterization tool, *Sediment. Geol.*, **347**, 36–52, (2017).

[33] Kramar, S., Lux, J.: Spectroscopic and porosimetric analyses of roman pottery from an archaeological site near Mosnje, Slovenia, *Mater. Tehnol.*, **49**, 503–508, (2015).

[34] Peyne, J., Gautron, J., Doudeau, J., Joussein, E., Rossignol, S.: Influence of calcium addition on calcined brick clay based geopolymers: a thermal and FTIR spectroscopy study, *Constr. Build. Mater.*, **152**, 794–803, (2017).

[35] Xie, J., Kayali, O.: Effect of initial water content and curing moisture conditions on the development of fly ash-based geopolymers in heat and ambient temperature, *Constr. Build. Mater.*, **67**, 20–28, (2014).

[36] Essaidi, N.: Formulation of aluminosilicate of geopolymer type based on Tunisian clays, in French, Doctoral dissertation, Limoges University, France, 2013.

[37] Rudolph, W.W., Irmer, G., Köninsberger, E.: Speciation studies in aqueous HCO_3-CO_3- solutions. A combined raman spectroscopic and thermodynamic study, *Dalton T.*, **8**, 900–908, (2008).

[38] Autef, A., Joussein, E., Gasgnier, G., Rossignol, S.: Parameters that influence silica dissolution in alkaline media, *Ceram. Eng. Sci. Proc.*, **33**, 13–24, (2012).

[39] Autef, A., Joussein, E., Poulesquen, A., Gasgnier, G., Pronier, S., Sobrados, I., Sanz, J., Rossignol, S.: Influence of metakaolin purities on potassium geopolymer formulation: the existence of several networks, *J. Colloid Interf. Sci.*, **408**, 43–53, (2013).

[40] Derrick, M.R., Stulik, D., Landry, J.M.: Infrared Spectroscopy in Conservation Science, Scientific Tools for conservation. The Getty Conservation Institute, Los Angeles, 1999.